

J. G. Gonzalez-Rodriguez · I. Rosales  
M. Casales · L. Martinez

## Corrosion resistance of molybdenum silicides in aqueous solutions

Received: 28 April 2004 / Revised: 20 October 2004 / Accepted: 23 November 2004 / Published online: 6 April 2005  
© Springer-Verlag 2005

**Abstract** The corrosion performance of Mo-22Si and Mo-25Si alloys in 0.5 M sodium chloride (NaCl) and 0.5 M sodium hydroxide (NaOH) solutions, at room temperature, was evaluated using electrochemical techniques. In 0.5 M NaCl, additionally, the effect of solution pH (3, 7 and 10) and concentration (0.1, 0.5 and 1.0 M) was studied using techniques such as potentiodynamic polarization curves, linear polarization resistance and electrochemical noise in current. The alloy contained either  $\alpha$ -Mo or Mo<sub>5</sub>Si<sub>3</sub> phases in a Mo<sub>3</sub>Si matrix. Polarization results showed that only the alloys containing 22Si developed a passive film in 0.5 M NaOH solution, whereas the alloy containing 25Si was passivated only in 0.5 M NaCl, pH 10 solution. In 0.5 M NaCl, pH 7 and 0.5 M NaOH solutions, the alloy with 25Si was the one with the highest corrosion rate, whereas the one containing 22Si was the most corrosion resistant. In NaCl solutions, the alloys exhibited a localized type of corrosion, but not in NaOH solutions. Alkaline NaCl solutions increased the corrosion rate of the 75Mo-25Si alloy with respect to acidic or neutral solutions, whereas diluted (0.1 M) or concentrated (1.0 M) NaCl solutions produced lower corrosion rates than the 0.5 M NaCl solution. Some localized type of corrosion occurred in the NaCl solutions, due to a selective corrosion of the  $\alpha$ -Mo and Mo<sub>5</sub>Si<sub>3</sub> phases with respect to the Mo<sub>3</sub>Si matrix.

**Keywords** Intermetallics · Molybdenum silicides · Mo<sub>3</sub>Si · Aqueous corrosion

### Introduction

Recently, research has focused on several kinds of materials, such as the intermetallic compounds based on Molybdenum silicides for their properties, i.e. mechanical and physical, due to the need for materials with good properties to support extreme conditions such as high temperature, high stresses, or corrosive environments. MoSi<sub>2</sub> is one of the most extensively studied compounds in the Mo-Si binary phase diagram, and, on the other hand, the only one with industrial application, due to an excellent resistance to the oxidation at high temperature as in elements of furnaces, for instance [1]. Two other compounds, Mo<sub>5</sub>Si<sub>3</sub> and Mo<sub>3</sub>Si, exist in this system.

It is very well known that, in the case of the MoSi<sub>2</sub>, its high temperatures oxidation stability is due to the formation of a highly protective SiO<sub>2</sub> layer which give them a high temperature degradation resistance, which was widely studied [5–7], this layer is formed neither in the Mo<sub>5</sub>Si<sub>3</sub> nor in the Mo<sub>3</sub>Si. However, the low temperature corrosion behavior of molybdenum silicides, such as Mo<sub>3</sub>Si, Mo<sub>3</sub>Si + Mo<sub>5</sub>Si<sub>3</sub> or Mo<sub>3</sub>Si +  $\alpha$ -Mo phases has not received much attention, with the exception of a few studies [8–11]. Thus, the aim of this work was to investigate the corrosion properties of these intermetallics in two commonly found environments: sodium chloride (NaCl) and sodium hydroxide (NaOH).

### Experimental procedure

Alloys with nominal silicon concentrations of 22 and 25 (at. %) were prepared by arc-melting of nominally pure elements in a partial pressure of argon, and drop-casting into water-cooled copper molds with a diameter of 12.5 mm. The two resulting alloys were 75(at.%) Mo-25Si and 78Mo-22Si. The specimens were annealed in a vacuum of 10<sup>-4</sup> Pa for 24 h at 1,600 °C, and then cooled using a cooling rate of 2.5 °C s<sup>-1</sup> between 1,600 °C and

J. G. Gonzalez-Rodriguez (✉) · I. Rosales  
UAEM, CIICAP, Av. Universidad 1001,  
62210 Cuernavaca,  
Mor., Mexico

M. Casales · L. Martinez  
UNAM, CCF, Av. Universidad S/N,  
62210 Cuernavaca,  
Mor., Mexico

1,000 °C and then furnace cooled. In order to compensate for the possible loss in Si due to evaporation, an extra 0.5 at. % of Si were added (since  $\text{Mo}_3\text{Si}$  is a line compound) to keep the final compositions of the alloys after the heat treatment in agreement to the Mo-Si alloy phase diagram. For the corrosion experiments, specimens of  $5 \times 5 \times 3$  mm were machined by an electro discharge machine, encapsulated in epoxy resin and then polished with diamond paste to a  $0.1 \mu\text{m}$  finish. Electrochemical experiments were performed using an ACM Instruments potentiostat controlled by a personal computer. Potentiodynamic polarization curves (PC) were obtained by varying the applied potential from  $-100$  mV with respect to the free corrosion potential,  $E_{\text{corr}}$ , up to  $+1,500$  mV at a rate of  $1$  mV/s. Before the experiments, the  $E_{\text{corr}}$  value was measured for approximately 30 min, until it was stable. All the potentials were measured using a saturated calomel electrode (SCE) as reference electrode. The counter electrode was a platinum wire. Corrosion rates were calculated in terms of the corrosion current,  $I_{\text{corr}}$ , by using linear polarization resistance curves, LPR, which was done by polarizing the specimen from  $+10$  mV to  $-10$  mV, respect to  $E_{\text{corr}}$ , at a scan rate of  $1$  mV/s, a standard scanning rate for this kind of experiment, to get the polarization resistance,  $R_p$ . Using the Stern–Geary equation, the  $I_{\text{corr}}$  value was calculated as follows:

$$I_{\text{corr}} = \frac{b_a b_c}{2.3(b_a + b_c)} \times \frac{1}{R_p}$$

where  $b_a$  and  $b_c$  are the anodic and cathodic slopes obtained from the PC. For the electrochemical noise in current (ECN) measurements, a zero resistance ammeter (ZRA), from ACM Instruments, controlled using a desktop computer, which also served to record the readings on floppy disks, was used. Time records consisted of blocks of 1,024 readings, taken at 1-s intervals, using a two electrodes arrangement. All tests were performed at room temperature ( $25 \pm 2$  °C). Solutions used included  $0.5$  M sodium chloride (NaCl), and  $0.5$  M sodium hydroxide (NaOH), which were prepared from analytical grade reagents. When necessary, the solution pH was adjusted by adding hydrochloric acid or NaOH. After the experiments, the specimens were cleaned to be observed in the scanning electronic microscope (SEM).

## Results

### Electrochemical tests

Polarization curves for the three alloys in neutral  $0.5$  M NaCl is given in Fig. 1. It can be seen that none of the alloys showed a passive region, only anodic dissolution. The most active free corrosion potential ( $E_{\text{corr}}$ ) values were for the alloy with high Si, e.g. 25Si, whereas the alloy with the lowest content in Si had the highest  $E_{\text{corr}}$

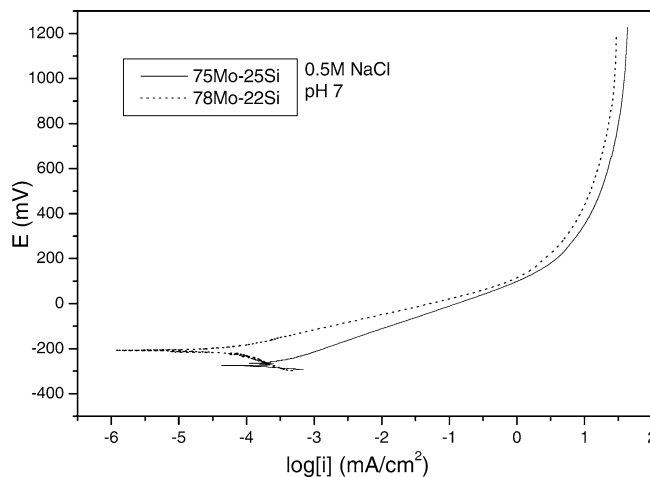


Fig. 1 Polarization curves for molybdenum silicides in  $0.5$  M NaCl

value. The anodic current density value was also highest for the alloy with 25Si, whereas the lowest value was for the alloy containing 22Si.]

Figure 2 shows the PC for the three alloys in  $0.5$  M NaOH. This time, the lowest  $E_{\text{corr}}$  value was for the alloy with 25Si, around  $-680$  mV, whereas the other alloy had an  $E_{\text{corr}}$  value around  $-500$  mV. Like in  $0.5$  M NaCl, none of the alloys showed a passive region, only anodic dissolution. However, the dissolution rates are quite high,  $0.1$  mA/cm<sup>2</sup>. The two alloys had very similar anodic current density values.

The effect of sodium chloride concentration on the polarization curve for the 75Mo-Si alloy is shown in Fig. 3. It can be seen that the  $E_{\text{corr}}$  values were virtually the same, showing no effect of the solution concentration. There was also a negligible effect on the anodic current density value, except at high anodic overpotentials, where it can be seen that the lowest anodic current density was for the most diluted solution, whereas the  $0.5$  M and  $1.0$  M solutions had very similar values. In none of these solutions the alloy

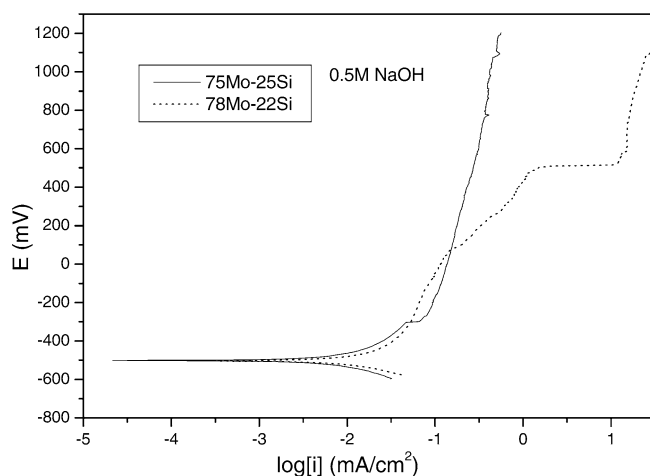
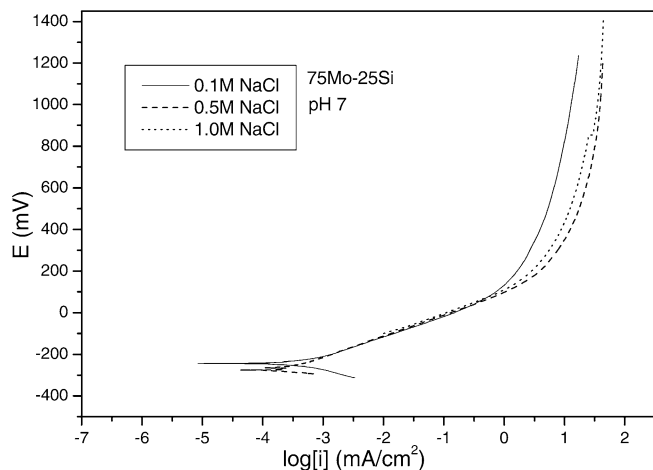


Fig. 2 Polarization curves for molybdenum silicides in  $0.5$  M NaOH



**Fig. 3** Effect of the NaCl solution concentration on the PC for the 75Mo-25Si alloy

showed a passive behavior but only anodic dissolution. Finally, the effect of the 0.5 M NaCl solution pH is shown in Fig. 4. It can be seen that the lowest  $E_{\text{corr}}$  value was for the most alkaline solution, around  $-600$  mV, whereas the noblest value was obtained in the acidic solution, around  $-220$  mV, 100 mV more anodic for the value obtained at pH 7. There was no passive region for this alloy except in a solution with pH 10, around 300 mV wide, with a pitting potential,  $E_{\text{pit}}$ , around  $-200$  mV, much lower than that obtained in 0.5 M NaOH solution, Fig. 2.

The change in  $I_{\text{corr}}$  with time for the three alloys in 0.5 M NaCl is shown in Fig. 5. It can be seen that the alloy with high Si contents, i.e. 25%, had a higher  $I_{\text{corr}}$  value than the one for the alloy with 22% Si. The two alloys tended to have constant  $I_{\text{corr}}$  values with time. In 0.5 M NaOH, Fig. 6, again, the alloy that had the highest  $I_{\text{corr}}$  value was the one containing 25Si, and the one with the lowest value, like in 0.5 M NaCl, was the one with 22Si. However, this time, the  $I_{\text{corr}}$  values never

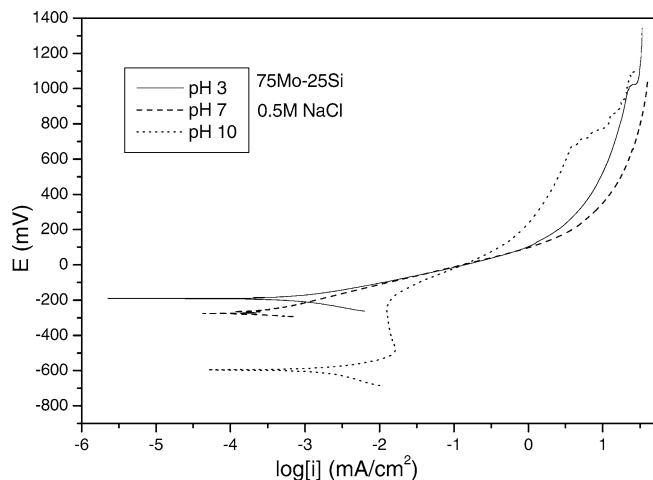


**Fig. 4** Effect of the NaCl solution pH on the PC for the 75Mo-25Si alloy

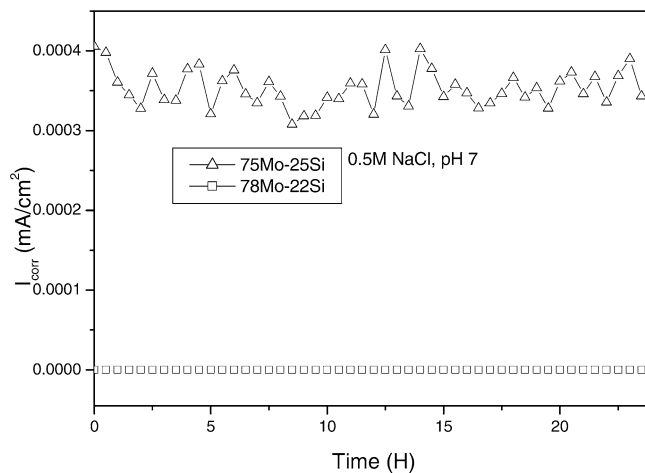


**Fig. 5** Change in  $I_{\text{corr}}$  with time for molybdenum silicides in 0.5 M NaCl

reached a steady-state value, like in 0.5 NaCl, instead, they tended to increase with time.

The effect of the 0.5 M NaCl solution pH in the  $I_{\text{corr}}$  values for the 75Mo-25Si alloy is shown in Fig. 7, where it can be seen that the lowest value was obtained in a solution with a pH value of 7. At the beginning of the test, the highest  $I_{\text{corr}}$  value was obtained in the most basic solution, at least during the first 10 h, however, after this time, this was reverted, and the highest  $I_{\text{corr}}$  value was obtained in the acidic solution, since the  $I_{\text{corr}}$  value in the alkaline solutions decreased with time, probably due to the presence of a passive film formed in this solution, as evidenced in Fig. 4. Finally, Fig. 8 shows the change in the  $I_{\text{corr}}$  value for the 75Mo-25Si alloy obtained at different NaCl concentrations. This figure shows that highest  $I_{\text{corr}}$  value was obtained in the 0.5 M solution, and the lowest value was obtained in the most diluted one, i.e. 0.1 M NaCl solution.

The results from the electrochemical noise experiments for 75Mo-25Si alloy in 0.5 M NaCl, pH 3 is

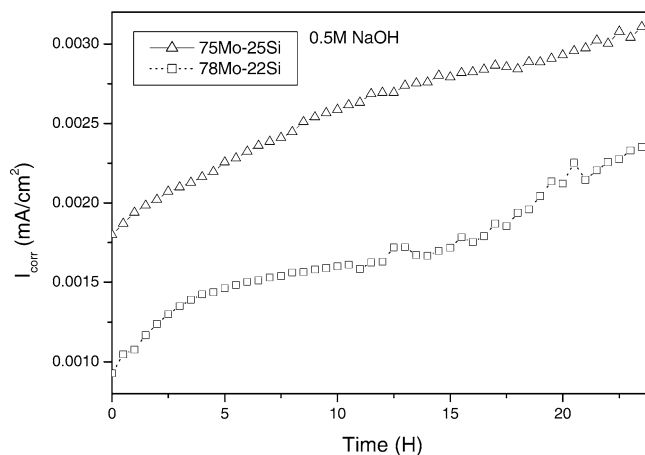


**Fig. 6** Change in  $I_{\text{corr}}$  with time for molybdenum silicides in 0.5 M NaOH

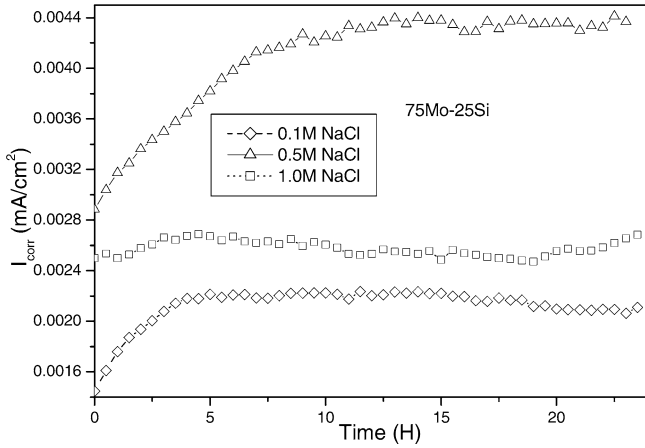


**Fig. 7** Effect of the NaCl solution pH on the change in  $I_{\text{corr}}$  with time for the 75Mo-25Si alloy

shown in Fig. 9, whereas the results of the tests at pH 7 are shown in Fig. 10. It can be seen that, in both cases, there are some anodic, (positive), and negative (cathodic) current transients, which are typical of some localized form of corrosion, such as pitting or crevice corrosion or even stress corrosion cracking [12–15]. The amplitude of the transients observed in the solution with a pH value of 7 was 100 times higher than those observed in the acidic solution. In 0.5 M NaOH, Fig. 11, on the other hand, the transients were of much higher frequency than the ones observed in NaCl solutions, but with lower intensity, which are typical of a material undergoing uniform corrosion, such as evidenced in the polarization curve for this solution in Fig. 2.

**Corrosion morphologies**

The microstructures of the two uncorroded alloys were described elsewhere [16], but briefly, the alloy containing

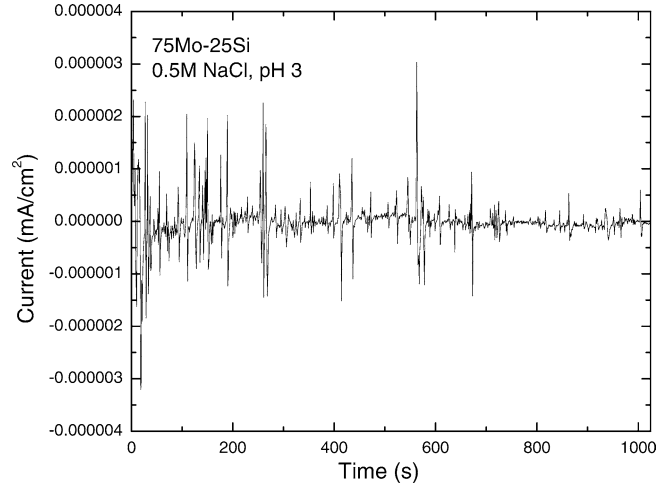


**Fig. 9** Electrochemical noise in current for Mo-25%Si in 0.5 M NaCl, pH 3

22 (at.%)Si contained  $\alpha$ -Mo precipitates in a  $\text{Mo}_3\text{Si}$  matrix specimen (Fig. 12), whereas the alloy with 25Si contained small particles of  $\text{Mo}_5\text{Si}_3$ , in a  $\text{Mo}_3\text{Si}$  matrix (Fig. 13). Small precipitates grew during the annealing process due to the evaporation of Mo. The grain size of the 25%Si was much larger than that for Mo-22%Si also.

Some typical micrographs of the corroded samples are shown in Figs. 14 throughout 16. Figure 14 shows the corroded surface of alloy Mo-25%Si in 0.5 M NaCl, pH 3 whereas the alloy with 22%Si corroded in this solution is shown in Fig. 15. In general terms, the phases with higher silicon contents were least corrosion resistant. For instance, in Fig. 14, it can be seen that the  $\text{Mo}_5\text{Si}_3$  phases were selectively corroded respect to the  $\text{Mo}_3\text{Si}$  matrix, whereas Fig. 15 shows that the  $\alpha$ -Mo phases were corroded preferentially respect to the  $\text{Mo}_3\text{Si}$ , matrix, as expected, due to the fact that Si imparts corrosion resistance to the matrix.

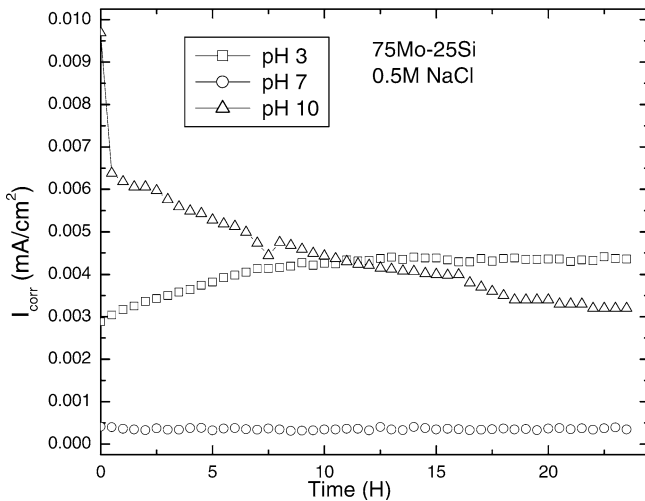


**Fig. 8** Effect of the NaCl solution concentration on the change in  $I_{\text{corr}}$  with time for the 75Mo-25Si alloy

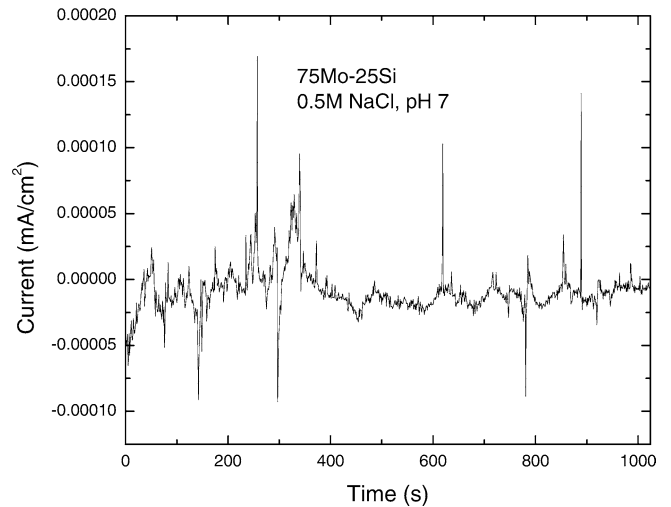


**Fig. 10** Electrochemical noise in current for Mo-25%Si in 0.5 M NaCl, pH 7



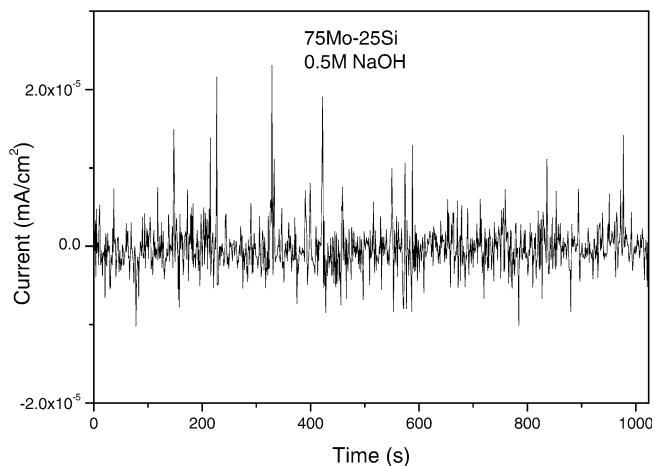


**Fig. 11** Electrochemical noise in current for Mo-25%Si in 0.5 M NaOH

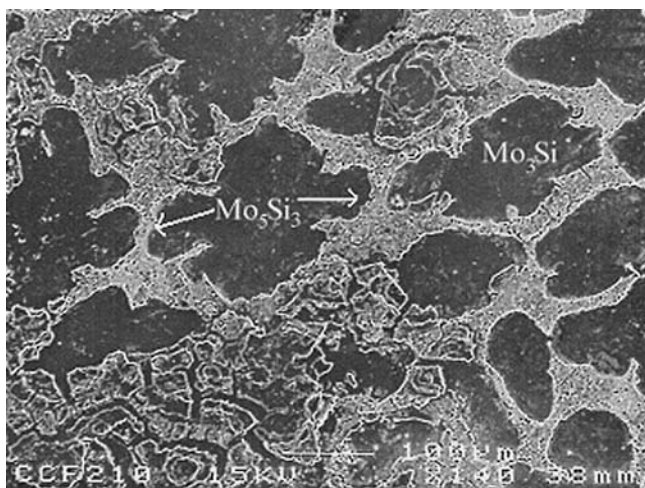


**Fig. 12** Surface morphology of the uncorroded Mo-22%Si alloy

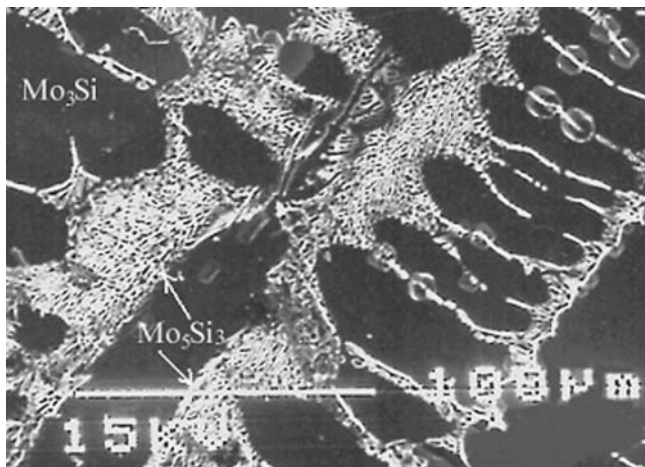


**Fig. 13** Surface morphology of uncorroded Mo-25%Si alloy

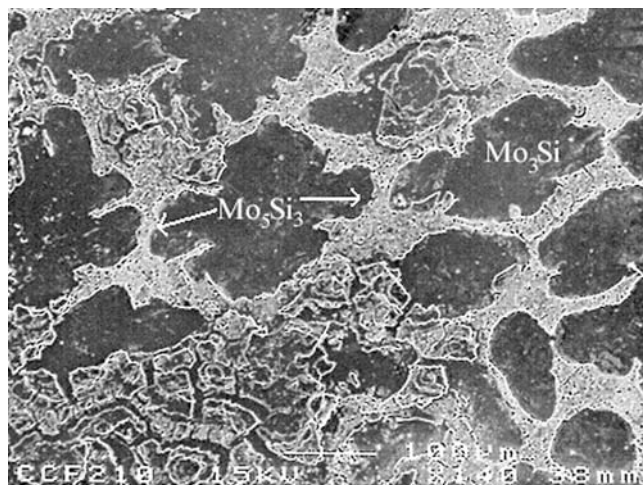


**Fig. 14** Surface morphology of Mo-25%Si in 0.5 M NaCl, pH 3

In 0.5 M NaCl, pH 7 solution, something very similar happened. For the alloy with 25%Si, for instance, as shown in Fig. 16, the  $\text{Mo}_5\text{Si}_3$  phases were preferentially corroded respect to the  $\text{Mo}_3\text{Si}$  matrix also.

## Discussion

It was clear that, in all cases, the alloy with higher silicon contents presented higher corrosion rate. Micrographs also showed that also, in all cases, for each alloy phases such as  $\alpha$ -Mo and  $\text{Mo}_5\text{Si}_3$  phases were always selectively corroded points respect to the  $\text{Mo}_3\text{Si}$  matrix, but there was not a direct relationship between corrosion rate and silicon contents since but they formed active galvanic cells with a large surface area. PC did not show the existence of a passive film on the alloy surfaces in either solution used, only anodic dissolution and solution diffusion through the corrosion products. ECN results showed the occurrence of localized corrosion for all alloys. Localized type of corrosion can take place only

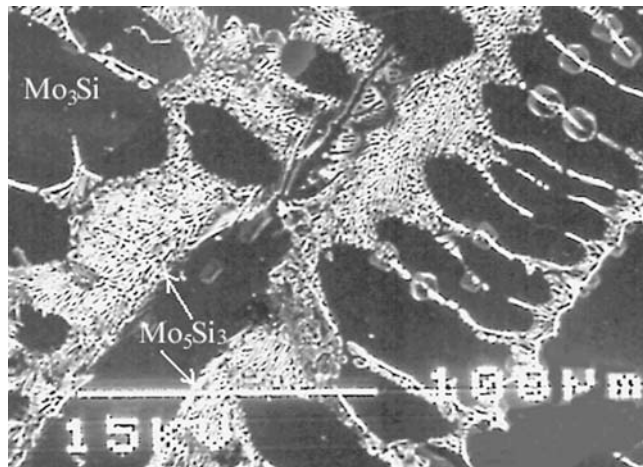


**Fig. 15** Surface morphology of Mo-22%Si in 0.5 M NaCl, pH 3

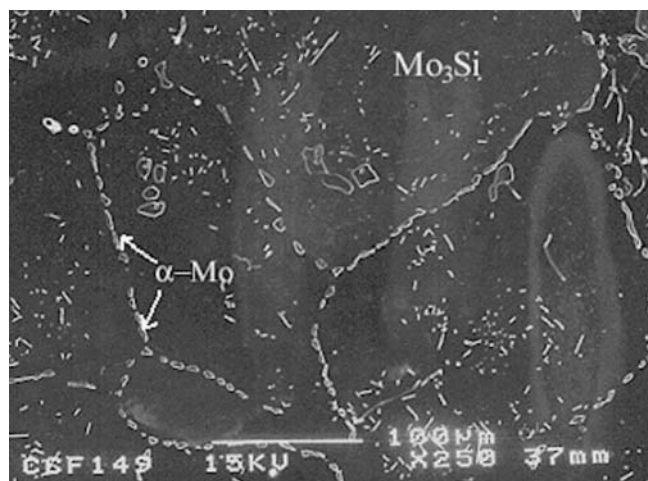


Fig. 16 Surface morphology of Mo-25%Si in 0.5 M NaCl, pH 7

with the disruption either of the passive film or the corrosion products barrier. Molybdenum silicides were studied intensively as their oxidation resistance results from the formation of a highly protective  $\text{SiO}_2$  layer in  $\text{MoSi}_2$ -containing alloys, and some authors have reported that the oxide film formed on these silicides upon anodic oxidation in aqueous solutions is similar to that obtained upon thermal oxidation [17]. Other authors [18] have concluded that no protective  $\text{SiO}_2$  film was formed on molybdenum silicides. Shams [17], when corroding  $\text{MoSi}_2$  anodically in acidic media found that the passivation could be due to the formation of hydrated oxides, whereas Halada [9], studying plasma-sprayed  $\text{MoSi}_2$  in sulfuric acid solution, reported that the passive film contained  $\text{SiO}_2$ , and exhibited a corrosion potential value of about  $-300$  mV. Our  $E_{\text{corr}}$  values here were from  $-250$  mV to  $-150$  mV in 0.5 M HCl and around 0 mV in 0.5 M  $\text{H}_2\text{SO}_4$ . Irrespective of the composition of the passive film, local disruption, either mechanically or chemically, will lead to localized corrosion.

In high temperature environments with high oxygen levels, it is believed that the sequential formation of  $\text{MoO}_3$  and  $\text{SiO}_2$  forms and passivate the surface [17], while in low oxygen molten salt applications, the low activity of phases such as  $\text{Mo}_5\text{Si}_3$  and  $\text{Mo}_3\text{Si}$  result in minimal corrosion [18].  $\text{MoO}_3$  volatilizes, which helps the  $\text{SiO}_2$  to establish continuity and hence protectiveness. This is only for  $\text{MoSi}_2$  and only in certain temperature ranges, usually around  $900$ – $1,000$  °C. As the temperature range used in aqueous environments precludes the formation of  $\text{MoO}_3$  and  $\text{SiO}_2$  and as Mo is only passive in a small pH range where  $\text{MoO}_2$  forms it is no surprise that these materials have high dissolution rates in solution. In comparison, Si is active at high pH according to the Pourbaix diagrams for both Mo and Si. Although the shape of the PC indicates the formation of a “passive” film on 22 Si in NaOH, the “passive” dissolution rates are quite high,  $0.1$  mA/cm<sup>2</sup>, this is not what one could call passivity and is likely the result of a Mo or Si precipitation reaction, but more research is needed to confirm this.

It is considered that the anodic transients are the result of a film rupture, which exposes the metal to the solution. The current transient is the result of exposure of the metal and their relatively slow current recovery reflects, perhaps, a repassivation process. The transient ceases on reformation of the film. The anodic transients observed suggest that these events are associated with an electron consuming reaction, cathodic discharge of the specimen. According to theoretical potential/pH ( $E/\text{pH}$ ) equilibrium diagrams [11] for Mo and Si, at the  $E_{\text{corr}}$  and the pH values of the solutions used here (from  $-250$  mV to  $-150$  mV in 0.5 M HCl and around 0 mV in 0.5 M  $\text{H}_2\text{SO}_4$ , and pH = 1), the two stable species are  $\text{MoO}_2$  and  $\text{H}_2\text{Si}(\text{OH})_6$ . So, molybdenum could be oxidized mainly to  $\text{Mo}^{4+}$  while silicide can be oxidized to silicic acid [18], which can be incorporated into the film. This film could contain, thus, both, molybdenum and silicon ions. The large area of the cathodic phase, i.e.  $\text{Mo}_3\text{Si}$ , together with a relatively small area of the anodic phases,  $\alpha$ -Mo and  $\text{Mo}_5\text{Si}_3$ , in combination with an aggressive environment, made conditions favorable for a selective corrosion of the least corrosion resistant phase to take place.

## Conclusions

The corrosion performance of Mo-22Si and Mo-25Si intermetallic alloys in NaCl and 0.5 M NaOH was evaluated using electrochemical techniques. Polarization results showed that only the alloys containing 22Si developed a passive film in 0.5 M NaOH solution, whereas the alloy containing 25Si was never passivated in any solution. In both 0.5 M NaCl, and 0.5 M NaOH solutions, the alloy with 25Si was the one with the highest corrosion rate, whereas the one containing 22Si was the most corrosion resistant. In NaCl solutions, the alloys exhibited a localized type of corrosion, but not in NaOH solutions. Some localized type of corrosion occurred in the NaCl solutions, due to a selective corrosion of the  $\alpha$ -Mo and  $\text{Mo}_5\text{Si}_3$  phases with respect to the  $\text{Mo}_3\text{Si}$  matrix. Alkaline NaCl solutions increased the corrosion rate of the 75Mo-25Si alloy with respect to acidic or neutral solutions, whereas diluted (0.1 M) or concentrated (1.0 M) NaCl solutions produced lower corrosion rates than the 0.5 M NaCl solution.

**Acknowledgments** The authors kindly acknowledge the experimental support of Dra. M. Casales from CCF-UNAM.

## References

1. Vasudevan AK, Petrovic JJ (1992) Mater Sci Eng A155:1
2. Meyer MK, Akinc M (1996) J Am Ceram Soc 79:938
3. Meyer MK, Akinc M (1996) J Am Ceram Soc 79:2763
4. Akinc M, Meyer MK, Kramer MJ, Thom JA, Huebsch JJ, Cook B (1999) Mater Sci Eng A261:16
5. Inoue T, Koike K (1978) Appl Phys Lett 33:826
6. Jiang H, Pettersson CS, Nicolet MA (1986) Thin Solid Films 140:115

7. Mochizuki T, Kashiwagi M (1980) *J Electrochem Soc* 127:1128
8. Urgan M, Stoltz U, Kirchheim R (1990) *Corros Sci* 30:377
9. Halada GP, Clayton CR, Herman H, Sampath S, Tiwari R (1995) *J Electrochem Soc* 142:74
10. Lu YC, Clayton RC (1989) *Corros Sci* 29:927
11. Herranen M, Delblanc Bauer A, Carlsson JO, Bunshah RF (1997) *Surface Coat Technol* 96:245
12. Hdlaky K, Dawson JL (1982) *Corros Sci* 22:231
13. Gabrielli C, Huet F, Keddam M (1986) *Electrochim Acta* 31:1025
14. Williams DE, Wescott C, Fleischmann (1984) *J Electroanal Chem* 180:549
15. Gonzalez-Rodriguez JG, Salinas-Bravo VM, Garcia-Ochoa E, Diaz-Sanchez A (1997) *Corrosion* 53:693
16. Rosales I, Schneibel JH, (2000) *Intermetallics* 8:885
17. Shams AM, El Din, Saleh RM, (1972) *Metalloberfl Angew Electrochem* 29:184
18. Jangg G, Kieffer R, Kögler H (1970) *Werkst und Korr* 9:699